

Research Article

Evaluation of Improving Water Flooding Technology by Volume Fracturing of Water Injection Wells in Complex Fractured Reservoirs: A Case Study of Chang 6 Reservoirs in Huaqing Oilfield, Ordos Basin

Shengping He ^{1,2}, Jiaosheng Zhang ^{1,2}, Chao Li,^{1,2} Xiqun Tan,^{1,2} Yi Ping,^{1,2} Desheng Li,^{1,2} and Jiang Chen^{1,2}

¹State Engineering Laboratory for Exploration and Development of Low Permeability Oil and Gas Fields, Xi'an 710018, China

²Research Institute of Exploration and Development, PetroChina Changqing Oil Field Company, Xi'an 710018, China

Correspondence should be addressed to Jiaosheng Zhang; zhangjs_cq@petrochina.com.cn

Received 30 May 2022; Revised 19 July 2022; Accepted 30 September 2022; Published 10 November 2022

Academic Editor: Dengke Liu

Copyright © 2022 Shengping He et al. This is an open access article distributed under the Creative Commons Attribution License, which permits unrestricted use, distribution, and reproduction in any medium, provided the original work is properly cited.

Given the problems of multiple natural microfractures developed in Chang 6 reservoir of Huaqing oilfield in Ordos Basin, the injected water flows along with the natural fractures during water injection development, resulting in low water drive recovery. The concept of volume fracturing is introduced into water injection well fracturing, and the technical idea of reconstructing the seepage field through volume fracturing of water injection well is proposed to improve the water flooding effect. On the basis of previous studies, firstly, the development of fractures and the rock mechanical properties of reservoirs are studied, and then the expansion law of volumetric fracturing fractures in the study area is analyzed. Combined with numerical simulation research, the feasibility of improving water drive by volumetric fracturing in water injection wells is demonstrated. Based on the above research, field tests of three well groups are carried out. The test shows that the volume fracturing of water injection wells can form a fracture zone along the direction of the maximum principal stress (with an average bandwidth of 56 meters), and then change the original dominant direction of water drive to realize the effective matching between fractures and injection production well pattern; the row spacing is reduced, and the effect of waterflooding is improved obviously. After the test, the average daily oil production of a single well increased from 0.6 tons to 1.0 tons, the water cut decreased from 74.6% to 42.0%. The oil recovery rate increased from 0.44% to 0.77%. The recovery increased by 5-8%.

1. Introduction

Chang 6 reservoir in Huaqing oilfield, Ordos Basin is a typical tight sandstone reservoir with low matrix permeability (the average permeability of surface gas measurement is $0.37 \times 10^{-3} \mu\text{m}^2$) and natural microfractures. The natural fractures not only improve the percolation capacity of low permeability reservoirs but also increase the risk of water channeling [1, 2].

The injection water channeling along natural fractures is very common in the development of complex fractured reservoirs. Chemical methods are generally used to improve the water drive effect in water shutoff and profile control. Especially in the ultra-low permeability reservoir with a complex fracture

network system, the effective period of water shutoff and profile control is short due to the difficulty of accurate identification of dominant channeling channels and the high requirements for the stability of chemical agents. According to statistics, the validity period of conventional water shutoff and profile control in Chang 6 tight sandstone reservoir is only 6-8 months.

Volume fracturing, also known as fracture network fracturing, is a technology to improve oil well production for tight reservoir development. Research and field tests show that the fracture zone distributed along the direction of the maximum principal stress can be formed through volume fracturing [3-7], which greatly improves the reservoir reconstruction volume, so as to improve the fracture control

degree of reserves and the ultimate EOR of the reservoir. Generally, small scale fracturing is used to solve the under-injection of water injection wells in low permeability oilfields [8–12]. Taking Chang 6 reservoir in Huaqing oilfield as the research area, this paper introduces the concept of volumetric fracturing into the water injection wells of ultra-low permeability complex fracture pattern reservoir and puts forward the technical idea of reconstructing the seepage field through volumetric fracturing of water injection wells to improve the effectiveness of water drive. By means of theoretical analysis and numerical simulation, it is proved that the technology of improving water drive by volumetric fracturing in water injection wells is feasible. The implementation of the field test and the achievement of good application effect prove that it has reference significance for the development of similar reservoirs.

2. Geological Background

2.1. Reservoir Characteristics

2.1.1. Petrology and Sand Body Characteristics. Huaqing oilfield is located in the middle of the Yishan slope in Ordos Basin, which is generally a gentle monocline and tends to the West. The main production layer is the Chang 6 oil layer of the Yanchang formation. The sedimentary microfacies belong to deep-water gravity flow. The width of the single sand body is 30–200 m, and the width thickness ratio is 30:1–50:1. The connectivity of the sand body on the plane is poor, and the mudstone interlayer is developed longitudinally. The lithology is mainly very fine-grained lithic arkose. The pore types are mainly micropores, dissolved pores, and intergranular pores, accounting for nearly 60% of the total pores, and intergranular pores are rare. It is a typical ultra-low permeability reservoir with average porosity of 11.5%, permeability of $0.37 \times 10^{-3} \mu\text{m}^2$, face rate of 3.8%, displacement pressure of 2.43 MPa, median pressure of 9.8 MPa, and median radius of 0.08 μm . The thickness and distribution of the oil layer are controlled by the sand body. The average oil layer thickness is 21.2 m.

2.1.2. Development Characteristics of Natural Fractures. Under the influence of the Yanshan and Himalayan tectonic movements, three groups of structural joints are developed in the Huaqing area, with the directions of 60° – 80° , 40° – 60° , and 100° – 110° (Figure 1). The fracture occurrence is mainly high-angle, and the dip angle is 65° – 85° , with an average of 79° . The natural fracture density is 0.74 pieces/m, the fracture opening less than 60 μm accounts for about 60%, the fracture spacing less than 6 cm accounts for about 80% (Figure 2), and the fracture depth less than 20 cm accounts for about 80%. Therefore, the natural fracture has the characteristics of “small opening, small spacing, and the small cutting depth”. Of these, 61% of natural fractures are unfilled.

2.2. Development Characteristics. From 2009 to 2012, advanced water injection was used to develop the Y 284 area of Chang 6 reservoir in the Huaqing oilfield, and the well pattern adopted is rhombic inverse nine points (480 m \times 130 m). The long diagonal direction of the diamond is NE 75° , which is consistent with the direction of the maximum principal

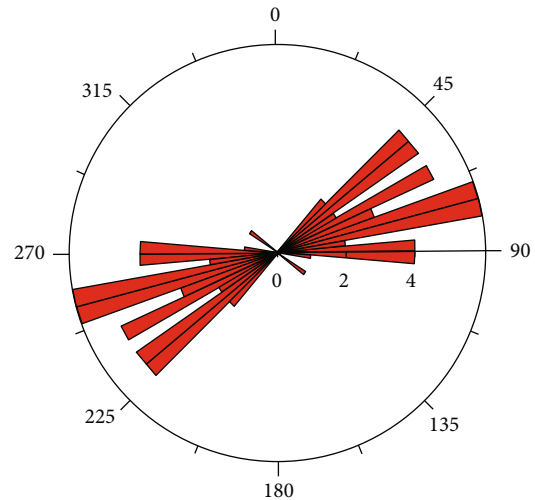


FIGURE 1: Statistics of fracture orientation observed in Chang 6 core.

stress of the reservoir. The oil production well is put into production after fracturing, and the water injection well is directly injected after perforation. By the end of 2018, the formation pressure remained at 92.3%, the injection production pressure reached 18.3 MPa, the water injection effective ratio was 45.7%, the water breakthrough ratio was 46.5%, the comprehensive water cut was 52.1%, the oil production rate of geological reserves was 0.2%, the recovery degree was 1.9%, and the overall water injection effect was poor. It can be seen from the water cut distribution map that most of the oil wells in the middle and north of the study area have been flooded along the main fracture direction, while the water cut in the south of the study area is relatively low (Figure 3). The analysis shows that the main factors affecting the effect of water injection development. The first one is the matrix permeability of the reservoir is low, therefore, the starting pressure gradient is large and the pressure conduction is slow. It is difficult to establish an effective displacement pressure system under the existing injection production well pattern. According to the statistics of well test data, the average pressure recovery rate is 1.0 MPa/100 h. After years of water injection, the injection production pressure difference increases year by year; the second is it is difficult to match the fracture network due to the development of natural fractures, and the injected water is easy to flow along with the natural fractures. The pressure difference between the main lateral oil well of the fracture is large (3–5 MPa), the main oil well is flooded rapidly, and the lateral oil well is ineffective for a long time. According to the tracer test and the study of the dynamic response characteristics of oil and water wells, the main water breakthrough directions are NW 45° , NW 75° , and NW 110° ; and the third is the vertical interlayer of the reservoir is developed, resulting in the low degree of production of water drive reserves.

3. Methods

3.1. The Feasibility Analysis of Volume Fracturing in Water Injection Wells to Improve Water Flooding. The rhombic inverse nine-point well pattern is used for water injection

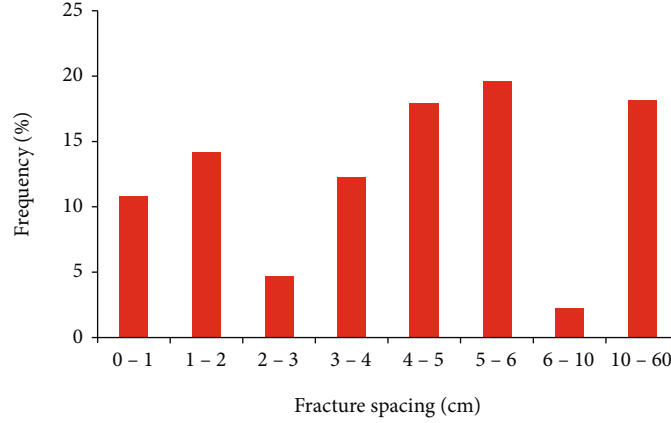


FIGURE 2: Frequency diagram of natural fracture spacing observed in Chang 6 core.

development in the study area. Only after fracturing of water injection well, the fracture extends along the long diagonal of rhombic, can the effective matching between fracture and injection production well pattern be achieved. This paper first discusses the influence of natural fractures on the extension direction of fracturing fractures, and then analyzes the extension direction of fracturing fractures after volume fracturing combined with the characteristics of the reservoir and in situ stress. On this basis, the seepage characteristics of water injection wells after volume fracturing are studied by using numerical simulation technology.

3.1.1. Analysis of Fracture Extension Direction of Volumetric Fracturing in Water Injection Wells. The research shows that the fracture extension of complex networks is affected by reservoir lithology, rock mechanical properties, geomechanics, and natural fracture characteristics. The main factors affecting the extension of fracturing fractures include the scale and properties of natural fractures, horizontal stress difference, approach angle, spacing between natural fractures and fracturing fractures, etc. [13–19]. Under high ground stress difference and large approach angle, hydraulic cracks will extend through natural cracks. Under low ground stress difference and small approach angle, natural fractures will open and change the direction of compressive fractures.

The maximum principal stress direction of Chang 6 in the Huaqing area is NNE, ranging from 65° to 90°, with an average of NE 75°, and the horizontal two-way stress difference is between 2.8–5.3 MPa. According to the relationship between the two-dimensional horizontal principal stress difference and the characteristics of fractures formed by fracturing [20] (Table 1), the analysis shows that the two-dimensional horizontal principal stress difference of Chang 6 is small, which is conducive to the formation of the fracture network system. Based on the experimental results of rock mechanical parameters of indoor core, the brittleness index of Chang 6 rock is calculated by using the modified Rick Rickman formula [21], and the result is 52%, which has strong compressibility (Table 2).

$$YM_{BRIT} = \frac{100 \times (YMS_C - 1)}{7 - 1}, \quad (1)$$

$$PR_{BRIT} = \frac{100 \times (PR_C - 0.4)}{0.15 - 0.4}, \quad (2)$$

$$BRIT = \frac{YM_{BRIT} + PR_{BRIT}}{2}. \quad (3)$$

YMS_C-static Young's modulus of rock, 10^4 MPa; PR_C-static Poisson's ratio of rock; BRIT-rock brittleness index.

Through the analysis of the key geological factors affecting volume fracturing, Chang 6 reservoir has a large brittleness index, small two-dimensional stress difference, and relatively developed natural fractures (density: 0.74 pieces/M), and has the geological basis for forming complex fractures. Since 2012, volume fracturing of two oil wells has been carried out in Chang 6 reservoir, and downhole microseismic fracture monitoring has been carried out. The results show that the fracture orientation is NE 75–81°. Taking Y297-61 as an example, the production horizon is Chang 6₃, and the effective sand body thickness is 25 m. It was put into operation in October 2009. In the initial stage, the average oil production of a single well was 2.3 t/d, and the average water cut of a single well was 11.4%. In October 2012, mixed water volume fracturing was carried out. The sand volume was 100m³, the sand ratio was 11.6%, and the displacement was 10m³/min. After fracturing, downhole microseismic monitoring was carried out. The orientation of the fracturing fracture was NE81° northeast, the bandwidth was 80 m, and the length was 465 m (Figure 4). After fracturing, the oil production of a single well increased from 0.7 t/d to 3.5 t/d, and the water cut was stable at 11.2%.

3.1.2. Seepage Characteristics after Volumetric Fracturing of Water Injection Wells. Numerical simulation is the preferred technical means to evaluate reservoir development effect, optimize reasonable development technical parameters, and tap the potential of remaining oil. Through numerical simulation, the reservoir seepage field and development indicators under different development modes can be simulated, so as to select the optimal scheme and ensure that the reservoir reaches a high development level. By establishing a three-dimensional two-phase black oil model to simulate the seepage field and development indicators before and after volumetric fracturing of water injection wells, this paper

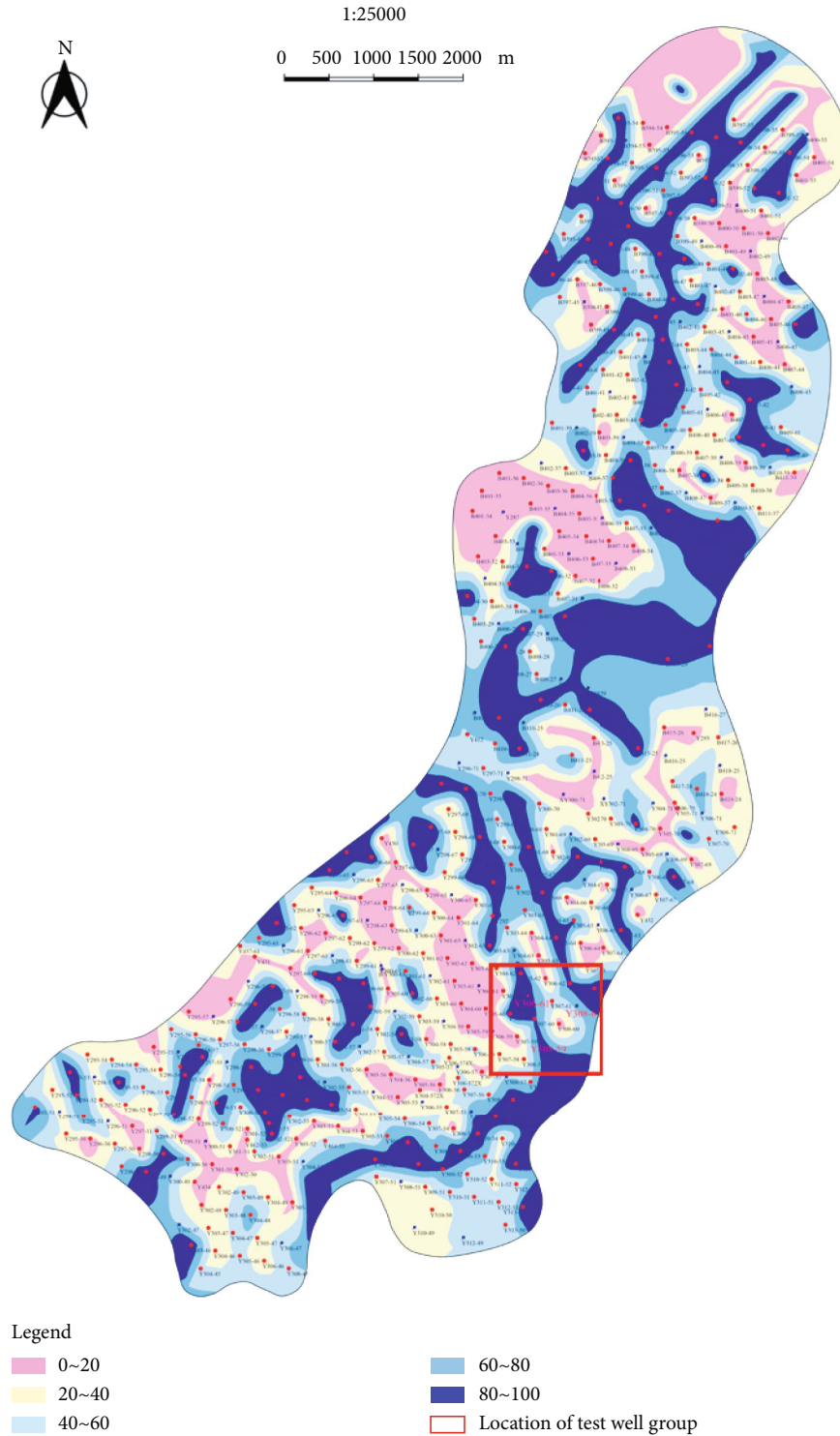


FIGURE 3: Water cut distribution in Y 284 area of Chang 6 reservoir in the Huaqing area.

TABLE 1: Fracture characteristics and realization difficulty of volume fracturing under different two-dimensional horizontal principal stress difference.

$(\sigma_H - \sigma_h)/\text{MPa}$	Fracture characteristics	Realization difficulty of volume fracturing
>10	Single crack	Large difficulty and small transformation volume
>5	Mainly single crack	Volume fracturing is difficult, and the reconstruction volume is small
<5	Volume crack	Easy volume fracturing and large reconstruction volume

TABLE 2: Mechanical parameters of sandstone in typical blocks of Ordos Basin.

Oil field	Coring layer	Number of coring wells	Number of cores	Young's modulus (MPa)	Poisson's ratio	Brittleness index (%)
Huaqing area	Chang 6	13	27	22577	0.22	52

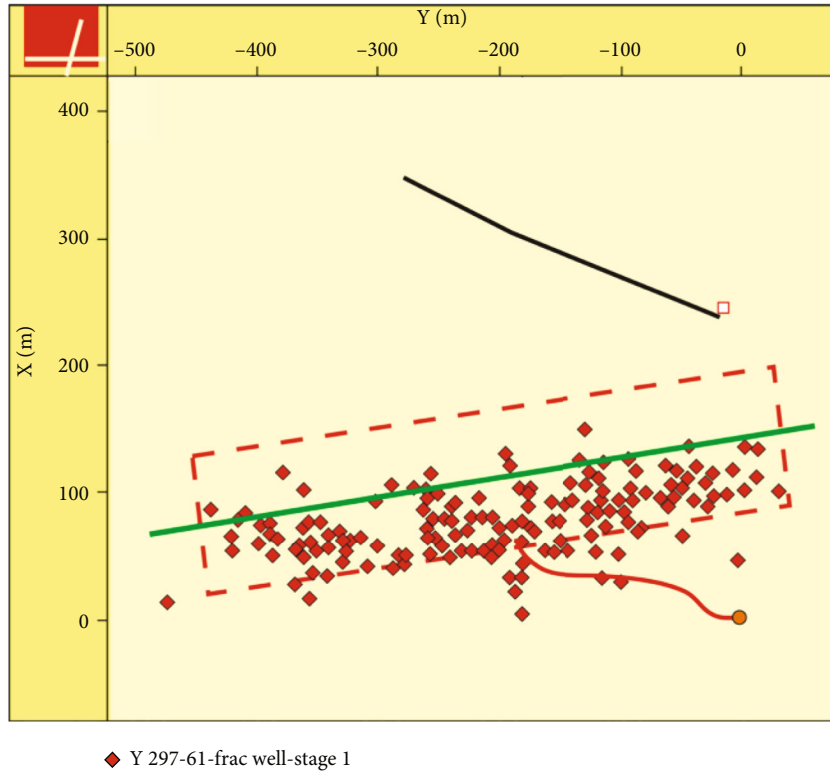


FIGURE 4: Top view of artificial fracturing in microseismic monitoring of well Y 297-61 of Chang 6 reservoir in Huaqing area.

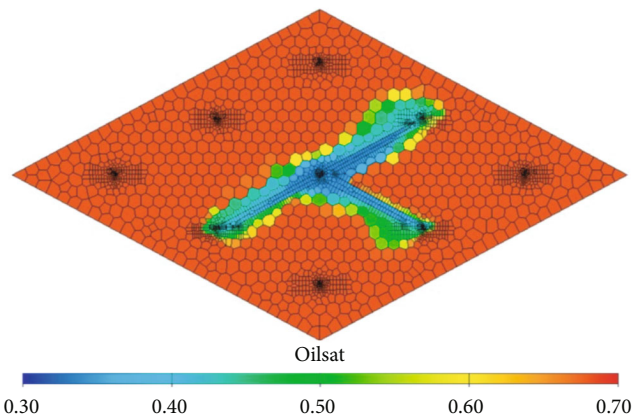


FIGURE 5: Distribution characteristics of seepage field in the 10-year period of the original development mode.

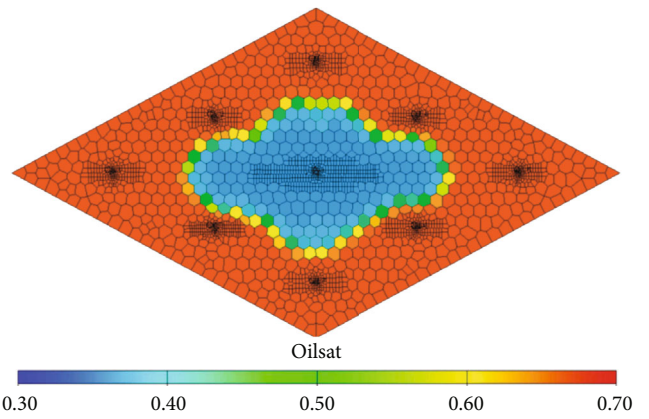


FIGURE 6: Distribution characteristics of seepage field in the 10-year period of volumetric fracturing transformation of water injection well.

demonstrates the feasibility of improving the development effect of well groups through volumetric fracturing of water injection wells.

The water breakthrough characteristics of the study area are multidirectional. The conventional right-angle grid and structured grid are difficult to deal with the water breakthrough problem of oil wells outside the orthogonal direc-

tion, especially the water breakthrough wells with violent water flooding fractures. PEBI grid has better flexibility. It does not only reduce the influence of the grid orientation effect on simulation results; but also has variable grid size, which can flexibly simulate fracture problems. It is the most effective means for fine characterization of complex fracture

TABLE 3: Fracturing construction parameters of test well group.

Well name	Layer	Perforated interval (m)	Sand quantity (m ³)	Sand ratio (%)	Displacement (L/min)	Breaking pressure (MPa)	Working Pressure (MPa)	Pump stop pressure (MPa)	Total liquid volume into the ground (m ³)
Y 308-59	Chang 6	2176.0-2184.0	50.0	11.7	8.0	27.9	24.7	20.5	531.1
		2191.0-2194.0							
Y 308-61	Chang 6	1941.0-1949.0	35.2	10.7	6.0	34.7	41.2	20.7	571.8
		1955.0-1961.0							
Y 306-611	Chang 6	1974.0-1980.0	25.1	12.1	6.0	33.6	39.7	18.1	446.2
		2112.0-2118.0	40.0	9.5	6.0	37.7	35.6	19.3	470.6
		2137.0-2144.0	20.0	9.0	6.0	36.0	34.8	18.8	252.8
Average		2146.0-2152.0	32.5	10.6	5.8	34.6	36.2	19.3	426.4

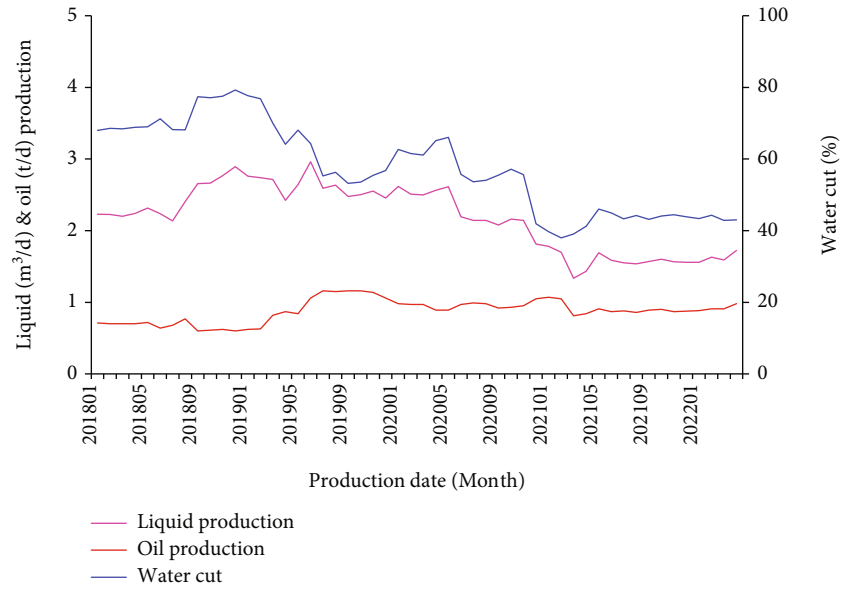


FIGURE 7: Production curve of test well group.

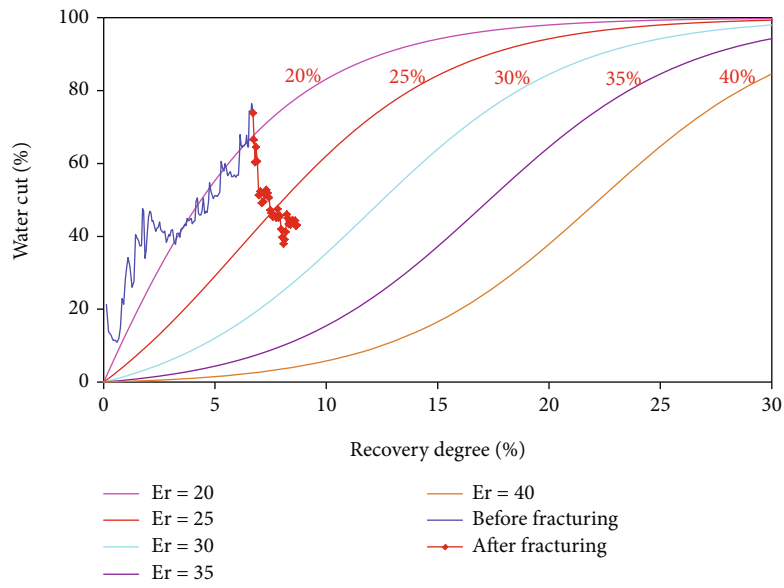


FIGURE 8: Curve of recovery degree-water cut of test well group.

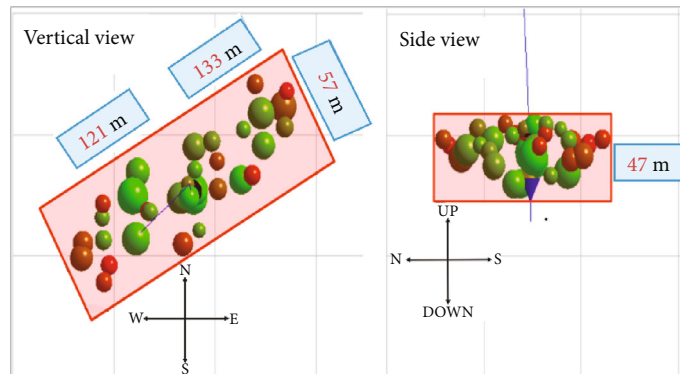


FIGURE 9: Test diagram of microseismic event of well Y 306-611(Chang 6₃¹⁻¹).

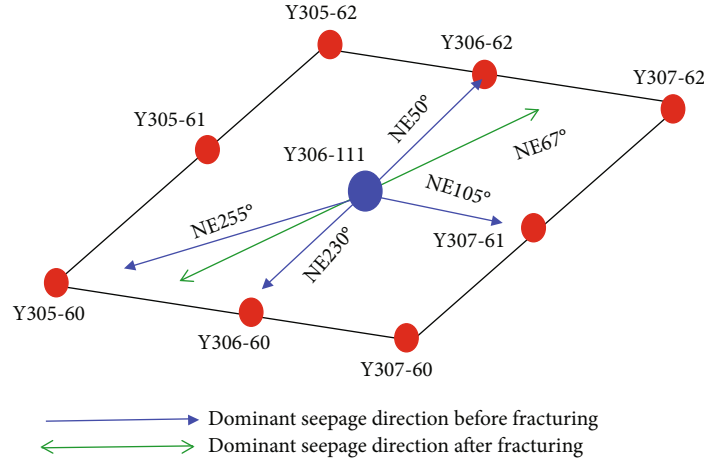


FIGURE 10: Schematic diagram of dominant seepage direction of water drive before and after fracturing of well cluster Y 306-611.

diversion reservoirs and volume fracturing seepage fields. The boundary of the PEBI grid system constructed by Unstructured Gridder is the constant pressure boundary. The permeability correction combined with skin coefficient method is used to treat the natural fractures and artificial fractures equally, and the anisotropy of formation permeability is considered at the same time. The main parameters of the model are: porosity is 11.5%, permeability is $0.37 \times 10^{-3} \mu\text{m}^2$, reservoir thickness is 20 m, artificial fracture half-length of production well is 80 m, bandwidth is 40 m, and conductivity is $10 \mu\text{m}^2\text{cm}$. Eight oil production wells and one water injection well are deployed, and the well pattern is rhombic inverted nine points ($480 \text{ m} \times 130 \text{ m}$). The production system adopts the dual control of limited target production and bottom hole flowing pressure.

The simulation results show that before the volumetric fracturing transformation of the water injection well, the water injection bursts along the fracture zone and the corresponding oil wells are flooded rapidly. The water injection well and three flooded wells form an invalid water injection cycle, and the five oil wells on the fracture side are ineffective for a long time, which results in a high production decline rate. The simulation predicts that after 10 years, the water injection swept width of fractured lateral wells is only about 50 m (Figure 5), and the recovery degree of well group is 2.86%. The water injection well is subject to volume fracturing after water plugging, and an artificial fracture network is formed along the long diagonal direction of the rhombic inverse nine-point well pattern. The artificial fracture of the water injection well is 180 m in half-length, 80 m in bandwidth, and $20 \mu\text{m}^2\text{cm}$ in diversion capacity for equivalent treatment. After the volume fracturing of the water injection well, the simulated seepage field is approximately elliptical along the direction of maximum principal stress. The corresponding 8 wells in the well cluster are basically uniform and effective (Figure 6). It is predicted that the recovery degree will reach 8.51% in 10 years. From the change of simulated seepage field and the comparison of development indexes, the volume fracturing of water injection well can better improve the water drive development effect of complex fracture ultra-low permeability reservoir.

3.2. Design of Field Test Scheme

3.2.1. Overview of Test Scheme. It is difficult to match well pattern and fracture pattern and establish effective displacement in Chang 6 complex fracture ultra-low permeability reservoir. By carrying out volume fracturing of water injection wells, reconstructing underground seepage fields, and changing the dominant direction of water drive, in order to improve the water drive effect. In this test, three well groups with stable sand body distribution, clear injection production correspondence, multi-directional water breakthrough, and clear water breakthrough direction are selected for the water injection well volume fracturing test. Before fracturing, the gyro inclinometer is used to verify the target coordinates. After fracturing, the downhole microseismic monitoring is carried out, and the water absorption profile is tested before and after fracturing. The purpose is to provide a basis for quantitative evaluation of the testing effect. A total of 11 support monitoring wells are carried out (including 6 gyro inclinometers, 4 water absorption profile tests, and 1 downhole microseismic monitoring).

3.2.2. The Design of Fracturing Parameter. According to the fracture criterion of Warpinski and Teufel and the two-dimensional linear elasticity theory, the net extension pressure in the joint required for shear fracture of rock mass is shown in

$$P_{\text{net}}(x, t) > \frac{1}{K_f} \left[\tau_0 + \frac{(\sigma_H - \sigma_h)}{2} (K_f - \sin 2\theta - K_f \cos 2\theta) \right]. \quad (4)$$

The net extension pressure in the joint required for tensile fracture failure is shown in

$$P_{\text{net}}(x, t) > \frac{(\sigma_H - \sigma_h)}{2} (1 - \cos 2\theta). \quad (5)$$

The net extension pressure in the joint required for rock body failure is shown in

$$P_{\text{net}} = -(\sigma_H - \sigma_h) + S_t. \quad (6)$$

TABLE 4: Production performance of single well before and after volume fracturing test of well cluster Y 306-611.

Production well	Tracer breakthrough time (d)	Tracer peak propulsion velocity (m/d)	Before test				At present				Contrast	
			Liquid production(m ³ /d)	Oil production(m ³ /d)	Water ratio(%)	Shut-in well for high water content	Liquid production(m ³ /d)	Oil production(m ³ /d)	Water ratio(%)	Oil production(m ³ /d)	Water ratio(%)	
Y 305-60	30	16.1	Shut-in well for high water content	Shut-in well for high water content	98.8	6.2	1.5	76.0	1.63	-20.7		
Y 306-60	42	6.5	6.1	0.1	98.8	1.2	0	100	0.11	-2.1		
Y 306-62	34	8.1	3.1	1.1	59.2	1.8	1.3	29.2	0.20	-30.0		
Y 307-61	4	68.5	4.4	0.5	87.7	1.3	0.7	50.0	0.21	-37.7		
Y 305-61	/	/	1.9	1.5	10.0	2.7	2.4	12.0	0.89	2.0		
Y 305-62	/	/	Shut-in well for high water content	Shut-in well for high water content	Shut-in well for high water content	Shut-in well for high water content	Shut-in well for high water content	Shut-in well for high water content	/	/		
Y 307-60	/	/	3.3	0.3	88.5	1.5	0.7	55.6	0.36	-32.8		
Y 307-62	/	/	2.2	0.8	56.2	1.2	1.1	10.6	0.28	-45.7		

P_{net} -net pressure of fracture extension during fracturing; K_f -friction factor of natural fracture surface; τ_o -core cohesion in natural fractures; σ_H -maximum horizontal principal stress; σ_h -minimum horizontal principal stress; θ -angle between natural crack and maximum principal stress; S_t -tensile strength of rock.

During fracturing, the “fracture net” system can be formed only when the net pressure in the main fracture meets Equations (4) and (5). During fracturing, the “fracture net” system can be formed only when the net pressure in the main fracture meets Equations (4) and (5). According to the rock mechanics and in situ stress parameters of Chang 6 reservoir, the fracture network system can be formed only when the fracturing displacement is greater than $5\text{m}^3/\text{min}$ combined with the practical experience of oil well volume fracturing, according to the technical idea of “large displacement, low sand ratio, and large liquid volume”. Comprehensively determine the fracturing construction parameters of the test well group, the displacement is $5\text{--}8\text{m}^3/\text{min}$, the sand ratio is $9\sim 12\%$, and the sand volume of a single well is $50\sim 60\text{m}$ (Table 3).

4. Results and Discussion

4.1. Overall Effect of Test. The test well group was put into operation in 2009 (Figure 3), including 3 water injection wells and 13 oil production wells (2 wells were shut down due to high water cut and 11 wells were in normal production). The volumetric fracturing test of the water injection well was started in December 2018. Before the test, the average liquid production of a single well was $2.9\text{m}^3/\text{d}$, the oil production was $0.6\text{t}/\text{d}$, the comprehensive water cut was 74.6% , and the recovery degree of geological reserves was 6.6% (Figure 7). At present, the average liquid production of a single well is $2.4\text{m}^3/\text{d}$, the oil production is $1.0\text{t}/\text{d}$, the comprehensive water cut is 42.0% , the oil recovery rate of geological reserves is increased from 0.44% to 0.77% , and the predicted oil recovery is increased by 8% (Figure 8).

4.2. Analysis of the Typical Well Groups. Taking well cluster of Y 306-611 as an example, there are 8 production wells in the well cluster (2 wells were shut down due to high water cut and 6 wells were in normal production). Before the test, according to the water absorption profile test, the water absorption capacity of Chang 6_3^{1-1} layer is weak; the water absorption profile of Chang 6_3^{1-2} shows a peak shape, and the relative water absorption accounts for 73% . The degree of water drive of well cluster is 75.8% . On the plane, according to the tracer monitoring results, the injected water can be seen in the oil production wells in the four directions of $\text{NE } 50^\circ$ and $\text{NE } 105^\circ$, etc. In December 2018, the volume fracturing of water injection wells was carried out, and the staged fracturing of Chang 6_3^{1-1} and Chang 6_3^{1-2} was carried out. The downhole microseismic monitoring showed that the fracture network was $240\text{--}254\text{m}$ long, $55\text{--}57\text{m}$ wide, and $43\text{--}47\text{m}$ high. The strike of the fracture network was $66\text{--}67^\circ$ North by East, which was basically consistent with the direction of regional principal stress (Figure 9). After volume fracturing, the relative water

absorption of Chang 6_3^{1-1} layer increased from 27% to 51% , the relative water absorption of Chang 6_3^{1-2} layer decreased from 73% to 49% , and the water driving degree of well cluster increased from 68.9 to 75.8% . On the plane, the dominant seepage direction is changed from $\text{NE } 50^\circ$ and $\text{NE } 105^\circ$ to $\text{NE } 67^\circ$ (Figure 10). From the production performance of production wells, the water cut of 4 production wells in the original dominant seepage direction decreased and the production increased (among them, the water cut of 3 wells decreased by more than 20 percentage points; the well of Y 305-60 shut down due to high water content, the oil production of single well reached $1.6\text{t}/\text{d}$ after the test.), and the daily oil production of lateral wells outside the original dominant seepage direction increased by 0.44t on average. The comprehensive analysis shows that the volume fracturing of the water injection well changes the formed dominant seepage direction and improves the production degree of longitudinal water drive. The fracture zone formed by fracturing improves the reservoir seepage energy and the water drive effect is significantly improved (Table 4).

5. Conclusions

- (1) The two-dimensional stress difference of the Chang 6 reservoir in the Huaqing area is small. The natural fractures are relatively developed. Theoretical research and field practice shows that the fracture zone extending along the direction of maximum principal stress can be formed through volume fracturing
- (2) The numerical simulation study shows that the volume fracturing of the water injection well can effectively improve the water swept volume and stage recovery degree. It is feasible to improve the water drive development effect of complex fracture ultra-low permeability reservoir by water injection well volume fracturing
- (3) The field test shows that after the volume fracturing of the water injection well, the effective matching between the fracture and the injection production well pattern is realized, the vertical production degree of the reservoir is improved, and the original dominant direction of water drive is effectively changed, and the water injection effect of the fracture lateral oil well is promoted. The overall oil increase and water cut reduction effect of the test well group is obvious. The technology of improving water drive by volume fracturing of water injection well has good adaptability to the reservoir with natural microfractures

Data Availability

The experimental data used to support the findings of this study are included in the manuscript.

Conflicts of Interest

The authors declare that there are no conflicts of interest regarding the publication of this study.

Acknowledgments

The authors would like to acknowledge the financial support from Major National Science and Technology Projects (2017zx05013-004); Major Projects of China Petroleum Science and Technology (2016e-0508).

References

- [1] Z. H. Xingui, Z. H. Linyan, and H. U. Chenjun, "Estimation of formation breakdown pressure and fracture open pressure of Chang 63 low permeable reservoir in Huaqing area and development suggestions[J]," *Journal of Central South University (Science and Technology)*, vol. 44, no. 7, pp. 2812–2818, 2013.
- [2] G. S. Cao, C. Tan, F. C. Song, Z. C. Qin, and W. W. Yang, "Pressure limit of enhanced water injection in low permeability oilfield[J]," *Science Technology and Engineering*, vol. 12, no. 13, pp. 3107–3110, 2012.
- [3] W. Xiaodong, Z. Zhenfeng, and L. Xiangping, "Mixing water fracturing technology for tight oil reservoir in Ordos Basin[J]," *Drilling and Production Technology*, vol. 34, no. 5, pp. 80–83, 2012.
- [4] WANG Yi, M. A. Xinfang, ZHANG Yong, and H. E. Jutao, "Optimization of volumetric fracturing parameters in the formation of Chang 8," *Science Technology and Engineering*, vol. 14, no. 29, pp. 189–193, 2014.
- [5] L. Jianshan, L. Hongjun, D. Xianfei et al., "Re-fracturing technology research and field application of mixing water volume fracturing in ultra-low permeability reservoir[J]," *Chemical Engineering of Oil and Gas*, vol. 43, no. 5, pp. 515–520, 2014.
- [6] W. A. Fei, Q. I. Yin, D. A. Yinpeng, and Y. A. Li'an, "Optimization of fracture network parameters of the wide zone SRV by old well in ultra low-permeability oil reservoirs," *Oil Drilling and Production Technology*, vol. 41, no. 5, pp. 643–648, 2019.
- [7] L. Xiangping, Q. Yin, L. Zhuanhong, H. Xinglin, and B. Jun, "Temporary plugging and mixed water volume fracturing technology of tight oil reservoirs in An83 block, Ordos Basin," *Petroleum Geology and Recovery Efficiency*, vol. 23, no. 6, pp. 120–126, 2016.
- [8] C. Zhongwen and C. Jun, "Fracturing technology of water injection well in the low permeability reservoir[J]," *Journal of Xinjiang Petroleum Institute*, vol. 13, no. 3, pp. 39–42, 2001.
- [9] Z. Lei, W. Wenjun, and Z. Hongun, "The numerical simulation research of water injection well fracturing in low permeability oilfield[J]," *P.G.O.D.D.*, vol. 22, no. 2, pp. 41–43, 2003.
- [10] D. Ren, L. Ma, D. Liu, J. Tao, X. Liu, and R. Zhang, "Control mechanism and parameter simulation of oil-water properties on spontaneous imbibition efficiency of tight sandstone reservoir," *Frontiers in Physics*, vol. 10, no. 10, article 829763, 2022.
- [11] D. Ren, H. Zhang, Z. Wang, B. Ge, D. Liu, and R. Zhang, "Experimental study on microscale simulation of oil accumulation in sandstone reservoir," *Frontiers in Physics*, vol. 10, no. 10, article 841989, 2022.
- [12] M. A. Bing, L. I. Xianwen, ZHENG Peng et al., "Study on interaction between hydraulic fracture and natural micro-fracture during the volume fracturing of tight oil reservoirs[J]," *Journal of Xi'an Shiyou University(Natural Science Edition)*, vol. 30, no. 2, pp. 44–48, 2015.
- [13] A. A. Daneshy, "Hydraulic fracture propagation in the presence of planes of weakness[C]," *SPE European Spring Meeting*, vol. SPE-4852-MS, pp. 1–8, 1974.
- [14] T. L. Blanton, "An experimental study of interactional between hydraulically induced and pre-existing fractures[C]," *SPE Unconventional Gas Recovery Symposium*, vol. SPE-10847-MS, pp. 559–571, 1982.
- [15] J. Zhou, M. Chen, Y. Jin, and G. Q. Zhang, "Experiment of propagation mechanism of hydraulic fracture in multi-fracture reservoir[J]," *Journal of China University of Petroleum*, vol. 32, no. 4, pp. 51–54, 2008.
- [16] F. Yao, M. Chen, X. D. Wu, and G. Q. Zhang, "Physical simulation of hydraulic fracture propagation in naturally fractured formations," *Oil Drilling and Production Technology*, vol. 30, no. 3, pp. 83–86, 2008.
- [17] N. R. Warpinski, M. J. Mayerhofer, M. C. Vincent, C. L. Cipolla, and E. P. Lolon, "Stimulating unconventional reservoirs: maximizing network growth while optimizing fracture conductivity[J]," in *SPE*, Keystone, Colorado, USA, 2008.
- [18] H. Wang, Z. Kou, D. A. Bagdonas et al., "Multiscale petrophysical characterization and flow unit classification of the Minnelusa eolian sandstones," *Journal of Hydrology*, vol. 607, article 127466, 2022.
- [19] G. Sheng, Y. Su, and W. Wang, "A new fractal approach for describing induced-fracture porosity/permeability/ compressibility in stimulated unconventional reservoirs," *Journal of Petroleum Science and Engineering*, vol. 179, pp. 855–866, 2019.
- [20] N. Potluri, D. Zhu, and A. D. Hill, "Effect of natural fractures on hydraulic fracture propagation[C]," *SPE*, vol. 94568, 2005.
- [21] R. Rickman, M. Mullen, and E. Petre, "Practical use of shale petrophysics stimulation design optimization: all shale plays are not clones of the Barnett shale[J]," in *SPE*, Denver, Colorado, USA, 2008.